aerospace

MDPI

Article

A Numerical Approach to Optimize the Design of a Pintle Injector for LOX/GCH4 Liquid-Propellant Rocket Engine

Jihyoung Cha *,†, Erik Andersson † and Alexis Bohlin

Department of Computer Science, Electrical and Space Engineering, Luleå University of Technology, Rymdcampus, Bengt Hultqvists väg 1, 98192 Kiruna, Sweden; erianq-6@student.ltu.se (E.A.); alexis.bohlin@ltu.se (A.B.)

* Correspondence: jihyoung.cha@ltu.se

† These authors contributed equally to this work.

Abstract: This study presents an optimal design approach of a pintle injector for a deep throttlable liquid-propellant rocket engine (LPRE). Even though the pintle injector is used in rocket engines, it has become more important since reusable launch vehicles (RLVs) recently became a trend due to their economic and environmental benefits. However, since many variables must be determined to design a pintle injector, optimizing the pintle injector design is complicated. For this, we design a pintle injector to optimize the performance parameters; the spray angle, vaporization distance, and Sauter mean diameter (SMD). To confirm the approach, we design a pintle injector using an optimization method based on convex quadratic programming (CQP) for a 1000 N thrust and a throttle ability of 5 to 1 LPRE with liquid oxygen and gaseous methane. Then, we verify the performance using a numerical simulation. Through this work, we check the effectiveness of the optimization method for a pintle injector design.

Keywords: optimal pintle injector design; optimization; convex quadratic programming; liquid-propellant rocket engine; numerical approach

Citation: Cha, J.; Andersson, E.; Bohlin, A. A Numerical Approach to Optimize the Design of a Pintle Injector for LOX/GCH4 Liquid-Propellant Rocket Engine. *Aerospace* **2023**, *10*, 582. https://doi.org/10.3390/aerospace10070582

Academic Editor: Justin Hardi

Received: 26 May 2023
Revised: 16 June 2023
Accepted: 21 June 2023
Published: 23 June 2023

1. Introduction

A pintle injector is one of the typical variable area injectors for a throttleable liquid-propellant rocket engine (LPRE) [1–3]. Although a pintle injector was developed in advance, a fixed injector was mainly used because most LPREs were disposable almost for delivering satellites to space, so only a maximum thrust was required, not an extensive throttle range. However, as the reusable launch vehicle (RLV) is one of the critical technologies in the new space age (sometimes space 2.0), a variable area injector has recently become essential as a next-generation injector because deep throttling is needed in a new LPRE for RLVs [4–7]. A pintle injector is an excellent option for a variable area injector required in a deep-throttling LPRE due to its relatively simple design, potential for high performance, and a high range of throttle. Moreover, the injector can minimize combustion instabilities, reducing manufacturing costs and increasing the propellant mixing potential [1–3].

For this reason, numerous research teams have studied the design and analysis of pintle-injector LPREs. However, they considered only the injection conditions and analyzed the performance under various injection conditions without optimizing the design studies [8–18]. Then, M. Son et al. introduced a design process that optimizes operation based on experimental results under various injection conditions [19]. After that, using Ref. [19], many researchers tried the optimal pintle injector design. B. Erkal et al. designed six different liquid oxygen and gaseous methane injectors for mission requirements and confirmed the performance by cold gas test [20]. R. Rajendran et al. also tried for an optimal pintle injector design and demonstrated it using a numerical approach [21]. However, they only designed several types of pintle injectors based on the approach of [19] with empirical

knowledge, not considering an optimization process, and determined their best design among those they designed by comparing each design performance.

Likewise, even though the pintle injector has several benefits, an optimal pintle injector design is challenging because of the many coupled design parameters and complicated design criteria. Furthermore, even after finishing a design process, the pintle operation must be tuned to ensure optimal performance in all thrust conditions. Therefore, this study suggests a simple optimization method for designing a movable pintle injector based on the relationship between the dimension and performance of a pintle injector in Ref. [19] and analyzes the impact of the optimal approach using a numerical simulation. To do this, we review the theoretical background considering a movable pintle injector and investigate the effect of performance by pintle injector design variables. Then, we optimize the design process using a convex quadratic programming (CQP) optimization approach for a pintle injector of a liquid oxygen and gaseous methane LPRE. Finally, we confirm the performance of the design approach using a numerical method and present our conclusions.

2. Theoretical Background

In this section, we present all underlying equations to predict a pintle injector performance and analyze the relationship between design and performance parameters. To simplify the calculation process, we consider an ideal LPRE using liquid oxygen and gaseous methane for a propulsion system [11,22] and review the relationship between the dimension and performance of a pintle injector using equations sourced from Refs. [19,23].

2.1. Pintle Injector

2.1.1. Concept of a Pintle Injector

A pintle injector for propellants with liquid oxygen and gaseous methane has a straightforward construct as illustrated in Figure 1 [19]. There is no area control used when injecting the gaseous propellant through an annular gap on the outside surface of the inner body, while a movable pintle in the middle controls the liquid propellant.

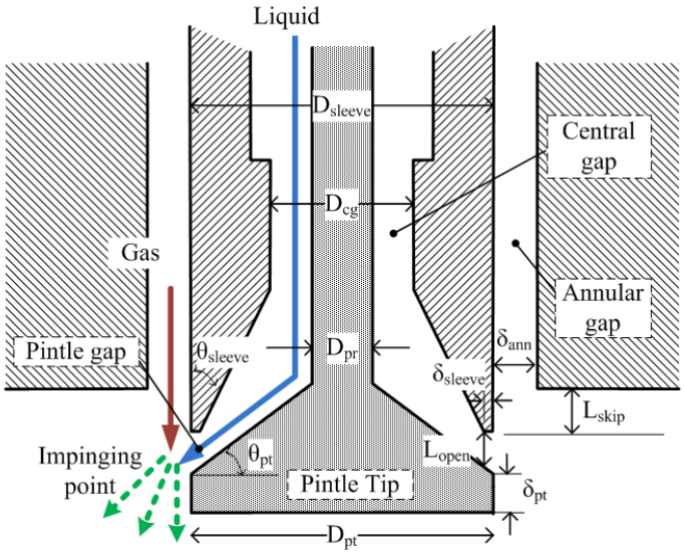

Figure 1. Schematic of pintle injector (Reprinted: Son, M., Radhakrishnan, K., Koo, J., Kwon, O. C., and Kim, H. D. Design procedure of a movable pintle injector for liquid rocket engines, 33(4), Copyright © 2016 by the American Institute of Aeronautics and Astronautics, Inc. with permission) [19].

One propellant is delivered through the outer flow tubes and then released to the combustion chamber (red arrow in Figure 1). The outlet propellant from the injector can be called the annular orifice as a flowing annular sheet in the line of the axis to the impinging point. The other propellant enters via a different central route to the pintle tip (shown as

the blue arrow in Figure 1). It changes to a uniform flow radially to the impinging point through the pintle gap after it hits the pintle tip. The pintle gap can change by the up and down movable pintle, so the central propellant exit area is controllable. This pintle injector controllability is beneficial because the control mechanism is quite simple to actuate the pintle. It gives the pintle injector a far greater throttle ability, ensuring combustion efficiency when comparing other types of injectors. However, although the pintle injector has a lot of strong points, it is challenging for a pintle injector design caused by many coupled and trade-off design variables with performance. Therefore, the design for a pintle injector should limit the scale of the design variables and consider the most important parameters [3].

2.1.2. Flows of Propellant

A mass flow rate ($\dot{m}$) can be described as

$$\dot{m} = \rho A U \tag{1}$$

where ρ, A and U are the propellant density, exit area of the orifice and fluid velocity, respectively.

The total propellant mass flow rate ($\dot{m}_{tot}$) can be expressed as

$$\dot{m}_{tot} = \frac{P_c A_t}{c^*} \tag{2}$$

$$\dot{m}_{tot} = \dot{m}_o + \dot{m}_f \tag{3}$$

$$OF = \frac{\dot{m}_o}{\dot{m}_f} \tag{4}$$

where p_c, A_t, c^*, $\dot{m}_o$, $\dot{m}_f$ and OF are the combustion chamber pressure, nozzle throat area, characteristic velocity, oxidizer flow rate, fuel flow rate and the oxidizer-to-fuel ratio, respectively.

Assuming that the liquid propellant is incompressible and the gaseous propellant is compressible, the velocity of each propellant can be calculated as

$$U_{liq} = C_{d,liq}\sqrt{\frac{2\Delta p_{liq}}{\rho_{liq}}} \tag{5}$$

$$U_{gas} = C_{d,gas}\sqrt{\frac{2R_{gas}T_{gas}\Delta p_{gas}}{\rho_{gas}}} \tag{6}$$

where C_d, Δp_{liq}, ρ_{liq}, R_{gas}, T_{gas}, Δp_{gas} and ρ_{gas} are the discharge coefficient of the orifice, the liquid propellant pressure drop across the injector, liquid propellant density and gas constant, injection temperature, pressure drop across the injector, and density of gaseous propellant, respectively.

2.1.3. Pintle Injector Dimensions

The pintle injector exit area (A_{pt}) can be calculated as

$$A_{pt} = L_{open}\pi\left(D_{pt} - 2\delta_{sleeve}\right) \tag{7}$$

$$L_{open} = \frac{L_{min}}{\cos(\theta_{pt})} \tag{8}$$

$$A_{min} = \pi\left(D_{pt} - 2\delta_{sleeve} - L_{min}\sin(\theta_{pt})\right) \tag{9}$$

where L_{open}, D_{pt}, δ_{sleeve}, θ_{pt}, L_{min} and A_{min} are the pintle opening distance, pintle tip diameter, pintle sleeve thickness, pintle tip angle, lower limit of the pintle opening distance, and minimum area between the sleeve and pintle tip, respectively.

The annular orifice area is given by

$$A_{ann} = \pi\left(\left(\delta_{ann} + \left[\frac{D_{pt}}{2}\right]\right)^2 - \left[\frac{D_{pt}}{2}\right]^2\right) \tag{10}$$

where A_{ann} and δ_{ann} are the annular orifice area and thickness of the annular gap.

2.1.4. Pintle Injector Performance

We can obtain the Sauter mean diameter (SMD), D_{32} as

$$D_{32} = L_{open}\xi^{-1}\exp(4.0 - q(We)^{0.1}) \tag{11}$$

$$q = 3.455 - 0.225\xi \tag{12}$$

$$\xi - \frac{90 - \theta_{pt}}{90} \tag{13}$$

$$We = \frac{\rho_{gas}L_{open}\left(U_{gas} - U_{liq}\right)^2}{\sigma_{liq}} \tag{14}$$

where ξ, We and σ_{liq} are the non-dimensional pintle tip angle, Weber number and liquid surface tension, respectively.

We can obtain the spray angle (α) using the total momentum ratio (TMR) as

$$\alpha = \cos^{-1}\left(\frac{1}{1 + TMR}\right) \tag{15}$$

$$TMR = \frac{\dot{m}_o U_o \cdot \cos(\theta_{pt})}{\dot{m}_f U_f + \dot{m}_o U_o \cdot \sin(\theta_{pt})} \tag{16}$$

In this study, we design a pintle injector with the fuel as the outer and oxidizer as the central propellant. Based on the arrangement, the vaporization distance (X) can be estimated using the following equations [23,24]:

$$X = r_{d0}^2\left[\frac{U_{d0}}{\sqrt{\gamma R_c T_c}} + \frac{3}{\Gamma}\cdot\frac{A_t}{A_c}\cdot\frac{\varphi}{10}\right]\cdot\frac{c_{p,c}\rho_o}{k_c}\cdot\frac{\sqrt{\gamma R_c T_c}}{\ln(1+B)}\cdot\frac{1}{2+\varphi} \tag{17}$$

$$\Gamma = \left(\frac{\gamma+1}{2}\right)^{\frac{\gamma+1}{2(\gamma-1)}} \tag{18}$$

$$B = \frac{c_{p,c}(T_f - T_c)}{h_{fg}} \tag{19}$$

$$\varphi = \frac{9}{2}\cdot\frac{Pr_c}{B} \tag{20}$$

where r_{d0}, A_c, $c_{p,c}$, k_c, T_f, h_{fg} and Pr_c are the initial droplet radius, the combustion chamber cross-sectional area, the specific heat capacity and thermal conductivity, the fuel temperature, the latent heat of vaporization, and the Prandtl number of the combustion gas, respectively.

The area can be obtained using a reasonable contraction ratio (A_c/A_t), generally, 13 for LPREs with a pintle injector [25].

2.2. Performance and Design Variables

There are many performance parameters to evaluate the performance of a pintle injector, so the selection and combination of the parameters are changed depending on the project requirement. In this study, we choose atomization, mixing, and vaporization distance as the performance parameters since the parameters are essential to maximizing the engine performance and can be influenced by the design of the injector outflow region. Then, we find the design variables of each performance parameter that strongly affect the performance.

2.2.1. Atomization

To evaluate the atomization performance of an injector, we should choose a valid method to express the droplets sprayed from the injector. Because the injector cannot generate a uniform size of droplets, using the average droplet size is an appropriate way for evaluation. In several methods, to evaluate the average size of the droplet, this study uses the Sauter mean diameter (SMD) since the SMD represents the average droplet size by the droplet diameter, where the surface-to-volume ratio of the droplets equals that of the entire spray [26]. Since the ratio is particularly interesting for the combustion process, the SMD can give information for the whole spray [24]. Therefore, we can evaluate the atomization performance by checking the SMD, where smaller diameters have better performance. Using the SMD equations (Equations (11)–(14)), we can also find the fundamental variables of the SMD. Keeping the thrust and pressure aimed, both pressure drops are fundamental variables because they directly affect the pintle injector exit area and pintle opening distance. Therefore, based on Equations (11)–(14), the relevant variables are the pintle tip diameter (D_{pt}), pintle tip angle (θ_{pt}), annular gap thickness (δ_{ann}), pintle pressure drop (Δp_{pt}), and annular orifice pressure drop (Δp_{ann}).

2.2.2. Mixing

Evaluating the mixing performance of an injector is challenging in a design process because the mixing performance only depends on the injector outlet fluid flow. Therefore, the best evaluation approach is a computational fluid dynamics (CFD) simulation, which makes the evaluation difficult and requires much time. For this reason, researchers have used guidelines to optimize the mixing performance at the beginning of the design. One is ensuring a uniform propellant distribution to the combustion chamber. Then, the pintle injector can offer good distribution. The spray can have a uniform propellant distribution by ensuring that the injector outlet fluid flow is as uniform as possible [22]. The other is to ensure the formation of recirculation zones in the combustion chamber, which is advantageous for mixing. Previous research shows that a larger spray angle increases the overall combustion performance and central recirculation zone [11,27]. Similarly, in the atomization case, both pressure drops are fundamental variables in keeping thrust and pressure aimed because they directly affect the pintle injector exit area and pintle opening distance. Therefore, using the spray angle, we can estimate the mixing performance of the injector. Similar to the atomization case, we can find the fundamental variables of the mixing performance based on Equations (15) and (16), which are θ_{pt}, δ_{ann}, Δp_{pt} and Δp_{ann}.

2.2.3. Vaporization Distance

The vaporization distance refers to the distance the average propellant droplet will travel before it is completely evaporated. By analyzing Equations (17)–(20), we can see that most variables depend on the propellants and the combustion process. For this, we assume that the impinging gas quickly accelerates the droplet, so the initial velocity of the droplet (U_{d0}) is the same as the injection velocity of the propellant, and the size of the initial droplet equals the SMD [23,28]. Through the assumption, the design variables can share with the SMD case, so the fundamental variables of the vaporization distance are also the same as the SMD case: D_{pt}, θ_{pt}, δ_{ann}, Δp_{pt} and Δp_{ann}.

2.3. Impact Evaluation

By finding the fundamental variables of the performance parameters, we determine the five variables to optimize the design: D_{pt}, θ_{pt}, δ_{ann}, Δp_{pt} and Δp_{ann}. After that, we analyze how the five design variables affect the performance parameters (SMD, spray angle, and vaporization distance). For this, we obtain the best oxidizer, fuel mass flow rate, and chamber pressure conditions considering the engine performance, such as combustion efficiency, characteristic velocity, and specific impulse, in each thrust for five design points using the CEA code and ideal rocket dynamic equations [22,29], described in Tables 1 and 2.

Table 1. Desired design points for each thrust level.

Thrust Level	Desired Thrust [N]	Characteristic Velocity [m/s]	Desired O/F Ratio
1	200	1854.4	2.6
2	400	1861.1	2.6
3	600	1865.4	2.6
4	800	1868.3	2.6
5	1000	1871	2.7

Table 2. Obtained design points for each thrust level.

Thrust Level	Calculated Thrust [N]	Chamber Pressure [bar]	Oxidizer Mass Flow [kg/s]	Fuel Mass Flow [kg/s]
1	200.9	5.9 (29.5% of max p_c)	0.0811	0.0312
2	398.9	9.4 (47% of max p_c)	0.1288	0.0495
3	602.6	13 (65% of max p_c)	0.1777	0.0683
4	794.7	16.4 (82% of max p_c)	0.2238	0.0861
5	1000	20 (max p_c)	0.2754	0.1020

Figure 2 indicates that increasing the diameter of the pintle tip decreases the vaporization distance and SMD, so a larger pintle tip diameter is better. Figure 2 also describes that the diameter does not affect the spray angle.

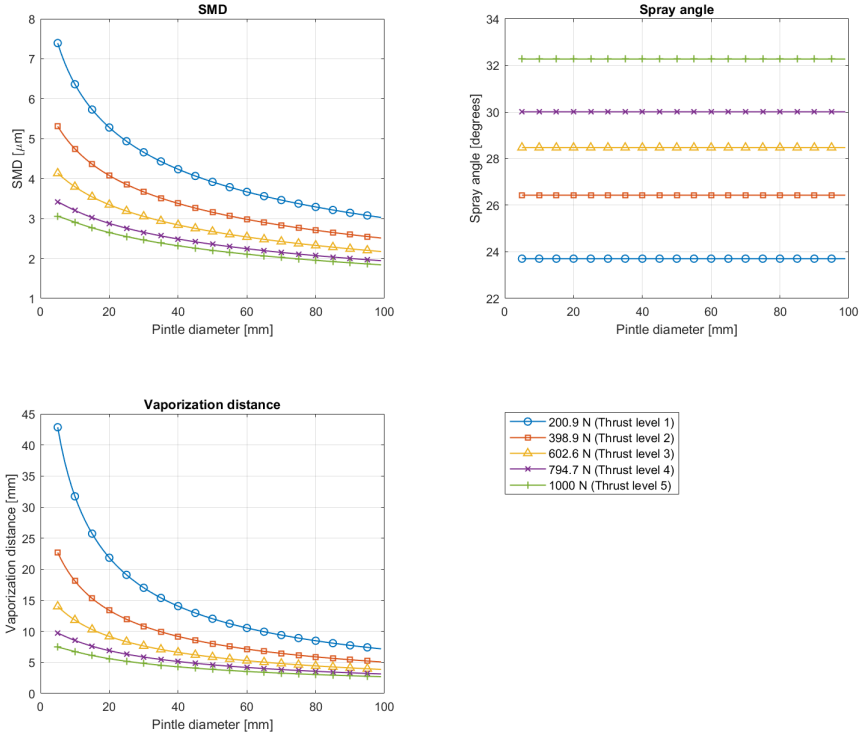

Figure 2. Effects of a pintle tip diameter on performance parameters: SMD, spray angle and vaporization distance.

Figure 3 shows that lower pintle tip angles are preferred based on three performance parameters. The SMD and vaporization distance increase as the pintle tip angle increases. It is not desirable because a smaller droplet size and smaller vaporization distance are better. The spray angle is also affected negatively since the spray angle decreases, which is undesirable, as the pintle tip angle increases.

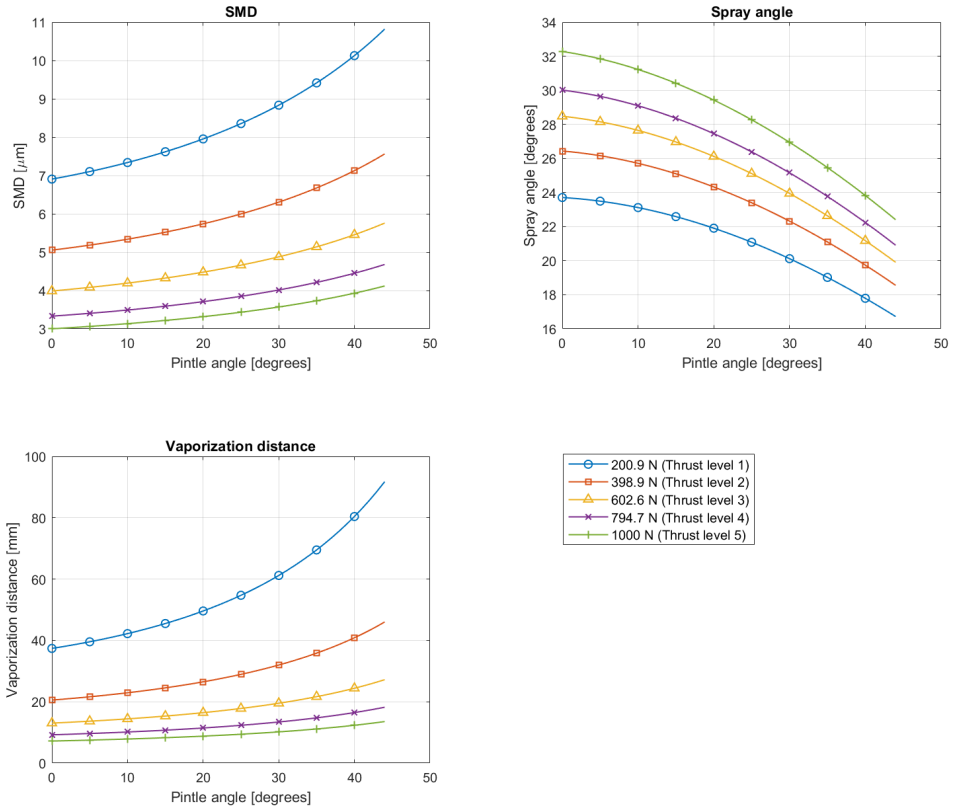

Figure 3. Effects of a pintle tip angle on performance parameters: SMD, spray angle and vaporization distance.

Figure 4 depicts that all performance parameters increase by increasing the annular gap. It benefits the spray angle but disadvantages the vaporization distance and SMD. Therefore, the annular gap depends on a specific project objective to optimize since negative and positive effects exist for the performance parameters.

Figure 5 shows an interesting vaporization distance and SMD trend. Increasing the pintle pressure drop decreases the SMD and vaporization distance at low thrust levels while increasing a bit at high thrust levels because increasing the pintle pressure drop decreases the pintle opening distance and Weber number, which have the opposite effect on the SMD and vaporization distance (Equations (11) and (17)). Hence, the SMD and vaporization distance converge to each value depending on the thrust level by increasing the pintle pressure drop. On the contrary, the spray angle increases monotonously by increasing the pressure drop. Therefore, similar to the annular gap case, the pintle pressure drop also depends on a specific project objective to optimize.

Figure 6 shows that all performance parameters decrease by increasing the annular pressure drop, which benefits the vaporization distance and SMD but disadvantages the spray angle. It indicates that a specific project objective decides the annular pressure drop as with the pintle pressure drop.

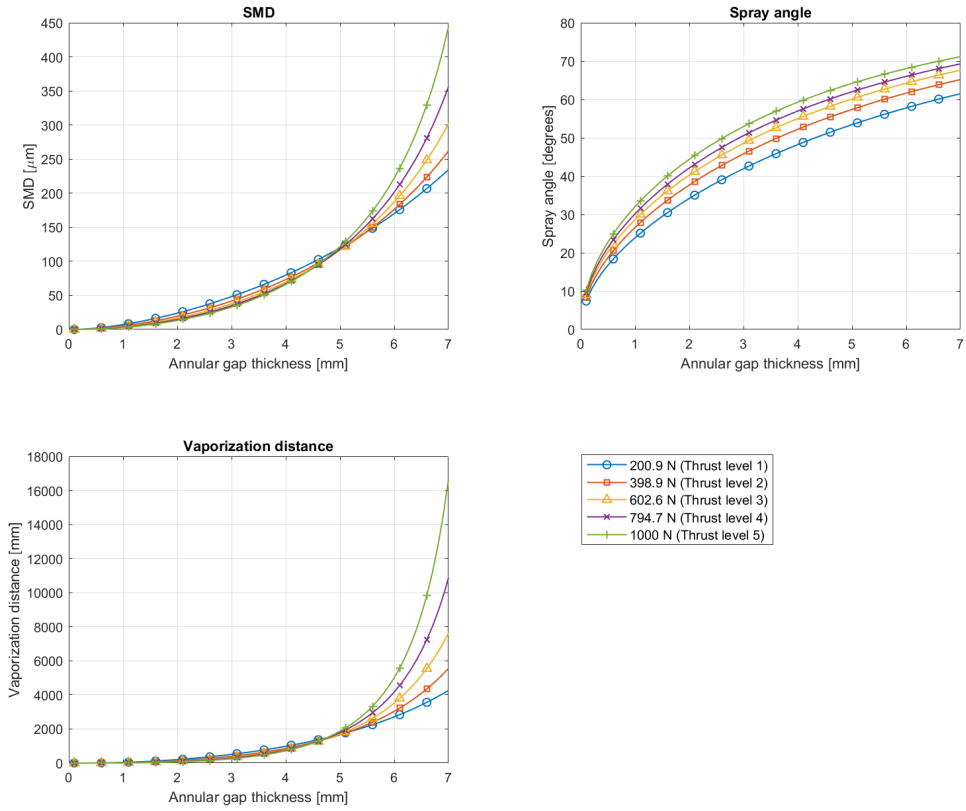

Figure 4. Effects of annular gap thickness on performance parameters: SMD, spray angle and vaporization distance.

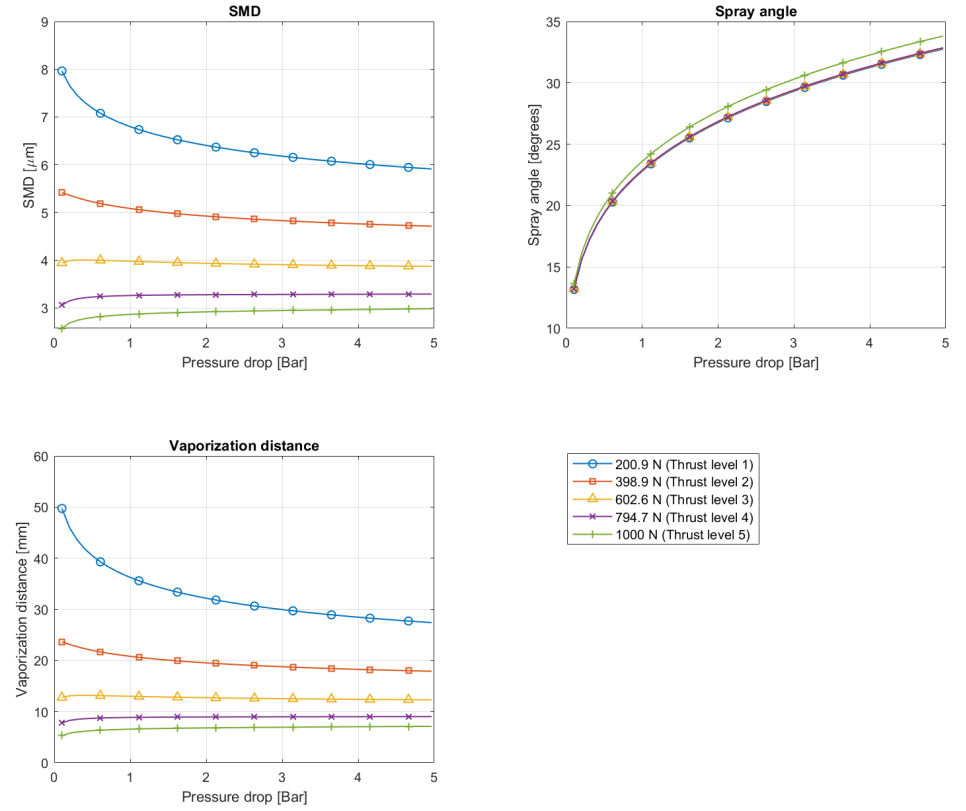

Figure 5. Effects of pintle pressure drop on performance parameters: SMD, spray angle and vaporization distance.

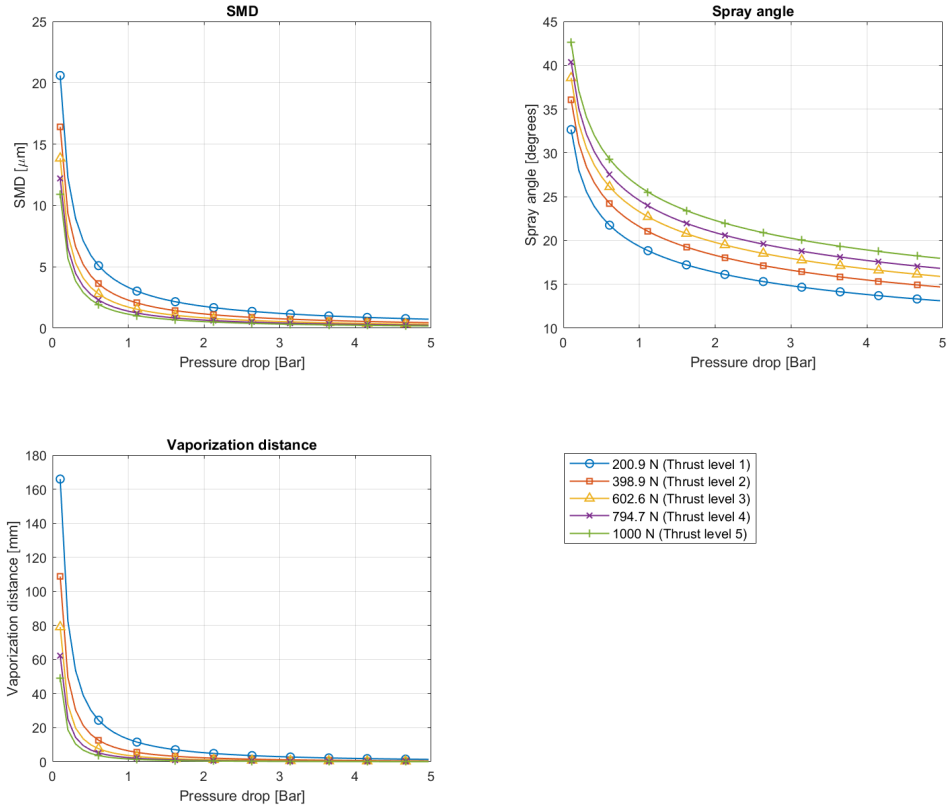

Figure 6. Effects of annular pressure drop on performance parameters: SMD, spray angle and vaporization distance.

We summarize the results in Table 3 based on the condition that maximizing the spray angle and minimizing SMD and the vaporization distance is desirable. The plus and minus signs in Table 3 denote whether a design variable affects each performance parameter positively or negatively. If a column only contains plus or minus signs, increasing the design variable affects the injector performance monotonously, so the variable should be maximized or minimized. However, there are some columns, including both signs. The column having both signs indicates that the performance impact of the design variables depends on a condition. It means that no one injector outflow region can be built in such a way as to offer the best performance for the whole set of performance criteria. Therefore, the injector design is determined by a specific project purpose.

Table 3. Summary of the design variable effects on the performance parameters.

	D_{pt}	θ_{pt}	δ_{ann}	Δp_{pt}	Δp_{ann}
SMD	+	-	-	+/-	+
X	+	-	-	+/-	+
α		-	+	+	-

3. Optimal Pintle Injector Design

3.1. Design Point

A pintle injector can be a control unit of a LPRE thrust control that directly affects the combustion conditions, so the pintle injector needs a wide operating range. Therefore, various optimal design points are required, while other injectors need only one point as shown in Figure 7 [23]. Generally, the characteristics of a pintle injector should be analyzed in various conditions with experience. For this, we analyze the characteristics in Section 2 using the equations of a pintle injector from Refs. [19,23] and design an optimal pintle

injector for a max thrust of 1000 N and a throttle ability of 5 to 1 with five optimal design points of a pintle injector as described in Table 2.

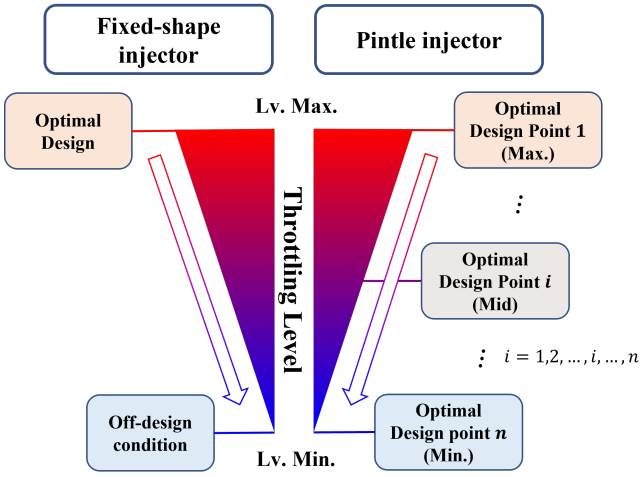

Figure 7. Comparison of optimal designs between the fixed injector and pintle injector (We modified pictures from M. Son's doctoral dissertation after receiving written permission from the author) [23].

3.2. Optimization Theory

The design is usually formulated into optimization problems to find the optimal design. There are many options for designing the optimization algorithm. In design optimization methods, a computer-aided numerical method is suitable for a system consisting of multiple coupled variables [30]. This study uses convex quadratic programming (CQP) to optimize the multivariate pintle injector design variables based on a cost function [31,32]. The method has several advantages for an optimal pintle injector design. First, the approach generates optimization problems that are typically easier to solve, and it ensures a unique global minimum, which is the best solution in the condition. It is also suitable for covering nonlinear conditions in a design process by applying the cost function or performance index. The cost function reflects the quality of the process, which can be modified easily to apply to various applications, so it is generally used in optimal control approaches to find the optimal condition maximizing performance with a constraint [30,33–38]. The cost function is shown as follows:

$$J = \mathbf{x}^T \mathbf{Q} \mathbf{x} = \begin{bmatrix} x_1 \\ x_2 \\ \vdots \\ x_n \end{bmatrix}^T \begin{bmatrix} Q_1 & 0 & \cdots & 0 \\ 0 & Q_2 & \cdots & 0 \\ \vdots & \vdots & \ddots & \vdots \\ 0 & 0 & \cdots & Q_n \end{bmatrix} \begin{bmatrix} x_1 \\ x_2 \\ \vdots \\ x_n \end{bmatrix} \tag{21}$$

where J is the cost or performance index of the optimization problem, x_i $(i = 1, 2, \cdots, n)$ is a state of the system, and Q_i $(i = 1, 2, \cdots, n)$ is a non-negative weight factor $(Q_i \geq 0)$. The optimal condition is when the cost is the minimum value as follows:

$$\min_{\mathbf{x}}(J) \Rightarrow \frac{\partial J}{\partial \mathbf{x}} = 0 \tag{22}$$

However, in the spray angle (α) case, it is desirable to maximize the state, unlike other performance parameters. Since the cost function in the QCP is designed to find the minimum value by modifying the cost function related to the spray angle, the condition of the maximum spray angle can be obtained when the modified cost function is minimal. Then, it can be combined easily with the cost function of the other performance parameters:

$$\max_{\mathbf{x}}(J_\alpha) \Rightarrow \min_{\mathbf{x}}(-J_\alpha) \tag{23}$$

$$\min_{\mathbf{x}}(J) = \min_{\mathbf{x}}(J_o) + \min_{\mathbf{x}}(-J_\alpha) \Rightarrow \min_{\mathbf{x}}(J_o - J_\alpha) \tag{24}$$

In addition, the F_{level} is added, considering the weight of individual thrust levels. In this study, we consider five optimal design points based on the thrust level, so we design better optimization at higher thrust levels because more efficiency at higher thrust yields more saved propellants. Therefore, the thrust weight factor is set corresponding to each thrust level ($\mathbf{x}_i$, J_i and $F_i = i$ for thrust level i, $i = 1, \cdots, 5$):

$$J = \sum_{i=1}^{5} F_i \cdot J_i = \sum_{i=1}^{5} F_i \cdot (J_{o,i} - J_{\alpha,i}) = \sum_{i=1}^{5} F_i \cdot \begin{bmatrix} D_{32} \\ X \\ \alpha \end{bmatrix}_i^T \begin{bmatrix} Q_D & 0 & 0 \\ 0 & Q_X & 0 \\ 0 & 0 & -Q_\alpha \end{bmatrix} \begin{bmatrix} D_{32} \\ X \\ \alpha \end{bmatrix}_i \tag{25}$$

Theoretically, because of the different orders of each performance parameter magnitude, each performance parameter should be normalization or non-dimensionalization, generally using each maximum aimed performance parameter. However, in this study, since there is not one design point but multiple design points, the factor of normalization or non-dimensionalization based on one specific design point can cause the weight factor effect changes in other design points. This paper focuses on introducing the optimization approach and showing the efficiency of the algorithm, so we apply the optimization algorithm performance parameters themselves without considering the normalization process.

3.3. Constraints of Design Variables

For the optimal design, we construct a cost function based on performance parameters D_{32}, X and α, considering the constrained critical design variables D_{pt}, θ_{pt}, δ_{ann}, Δp_{pt} and Δp_{ann}. Using the CQP, we can find the best injector design variables by minimizing the cost consisting of the performance parameters. We consider the constraints of the variables for better performance. For this, we investigate major previous research [10–14,16,19,23,25,39] and set the constraints based on the research as follows:

- D_{pt} should be in the range between 5 mm and 100 mm because a smaller pintle tip is hard to manufacture, and a larger tip is excessively large in this study.
- δ_{ann} should be in the range between 0.01 mm and 6 mm since a smaller annular gap thickness is hard to manufacture, and a larger gap is excessively large in this study.
- L_{open} should be larger than 0.1 mm since Ref. [19] found that an opening distance lower than the limit can cause formation trouble of a uniform liquid sheet outside the pintle tip.
- $\Delta p / p_c$ should be in the range between 0.05 and 0.3. This ratio is generally set at around 20% based on a rule of thumb. A higher value means more expensive pressure machinery and a lower value causes negative effects, such as chugging. Ref. [40] demonstrates engines with a 5% pressure ratio, so we determine the ratio as the lower limit.
- The velocity of propellant injection should be slower than the sonic velocity. It is not desirable because the supersonic injector rockets are less efficient than the sonic injectors and produce less thrust per unit mass flow [41], and the combustion chamber can be highly harmful when a supersonic flow is present because it cause high pressure and shock wave [42–44].

Considering the constraints, the optimization approach can be utilized by selecting the $\mathbf{Q} = \mathrm{diag}(Q_1, \ldots, Q_i)$ in Equation (25). The selecting Q_i values impact each performance parameter, so the user should find the proper $\mathbf{Q}$ values and assess which weights are appropriate for the specific project objective to optimize the pintle injector. The overall procedure of the optimization is described in the flowchart as shown in Figure 8.

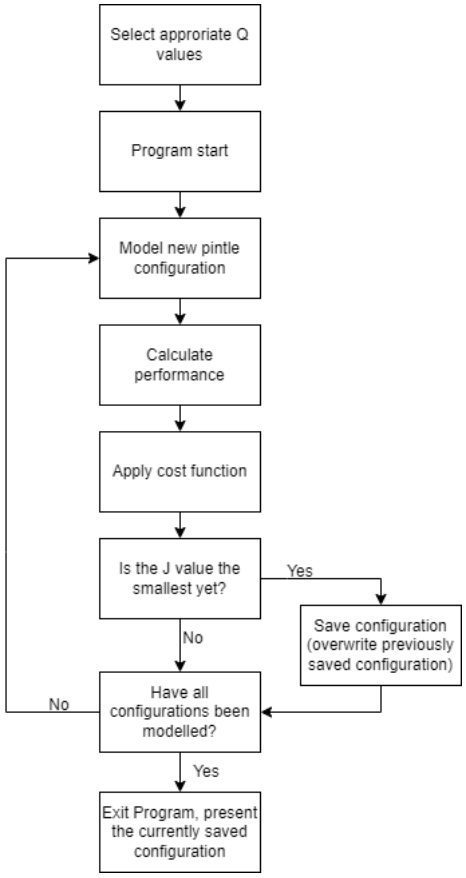

Figure 8. The optimization process flowchart.

3.4. Analyze the Weight Factor Impact

In the optimization process, since the design variables change depending on the weight matrix (**Q**), we use a graphical approach to investigate the impact of **Q** on the results of the optimization algorithm by constructing a set of surface plots. The horizontal axes are two of the Q_i ($i = D$, X, and α) value changes, and the vertical axis is each performance parameter of the optimized injector. Since there are three Q_i values, we analyze the impact by changing a pair of Q_i values in the case without considering normalization or non-dimensionalization and keeping with the other Q_i value of 1 in each plot.

The results are described in Figures 9–11 for the SMD, spray angle, and vaporization distance, respectively. As in Equation (25), the Q value of the spray angle has a negative effect while the other Q values have a positive effect. The results in Figures 9–11 generally show a sloping area with flat portions along the slope. The flat regions arise when the optimization method encounters the constraint of the design variables in Section 3.3, and the Q_i values are saturated. Therefore, the Q_i values should be located on the value of the sloping area because the region is the place where different weights affect the performance parameters significantly. The results show that the Q_i values, approximately in the range of 0.1 to 10, make the results of the performance parameters on the slope, so the weight values in the range can be regarded as reasonable. However, values at the ends of the range should be used with caution because they may cause the method to be saturated by the other chosen Q_i values. Through this work, we can find optimal pintle injector design variables using the algorithm.

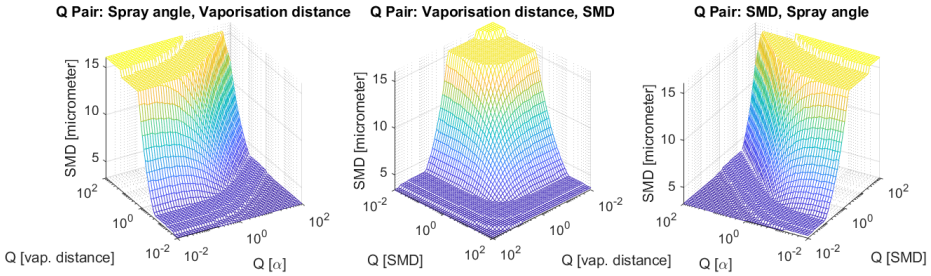

Figure 9. The effect results of SMD by the weight factors.

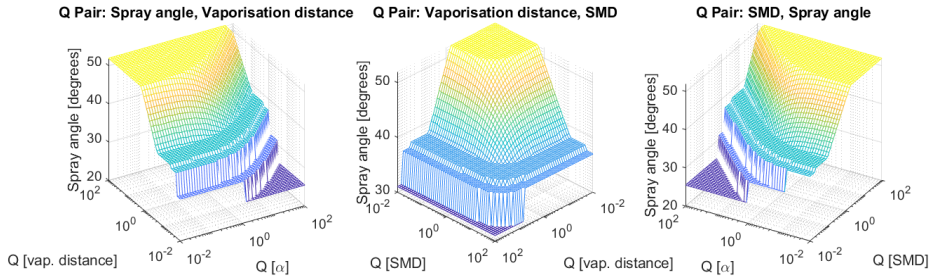

Figure 10. The effect results of the spray angle by the weight factors.

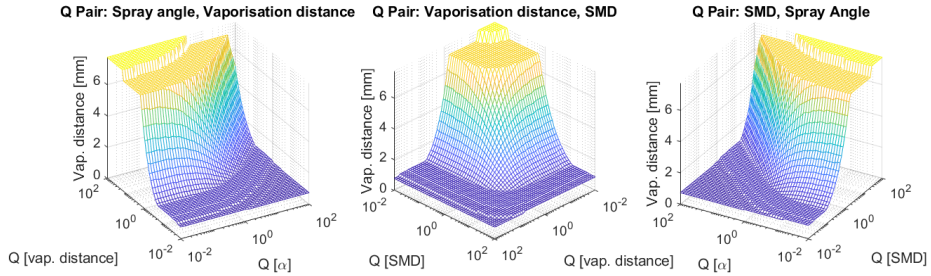

Figure 11. The effect results of the vaporization distance by the weight factors.

4. Verification and Discussions

Choosing the final configuration is essential because the weight factors are critical for the injector design. Generally, the biggest weight factor is placed on the most important performance parameters. Since this study has no emphasis on a specific performance, we choose the balanced Q_i values reasonably. However, because of the significant impact on combustion performance, we put slight weight values on the SMD and vaporization distance. Therefore, we determine the Q_i values to generate an injector by focusing on smaller SMD sizes without neglecting the vaporization distance and spray angle. The final design variable results and theoretical results of the performance parameters are illustrated in Tables 4 and 5.

Even though Table 5 represents the optimized injector performance by the design optimization process, we should validate the SMD, spray angle, and vaporization distance results because the performance in Table 5 is the theoretical results. However, droplet generation and vaporization are difficult to model accurately. On the contrary, the spray angles can be modeled assuming that a combustion effect and vaporization are negligible. Since the spray angle only depends on TMR, this assumption can provide accurate results, so we use a numerical simulation by COMSOL Multiphysics 2D axisymmetric simulation with a multiphase model and multiple domains to verify the spray angle [45]. Figure 12 shows the results of the spray angle simulations and excellent matches with the theoretical results in Table 5. Therefore, it shows that the calculated values are accurate, and the pintle injector design using the optimization method is reasonable and effective.

Table 4. The design variable results from the optimization process for a pintle injector ($Q_D = 2$, $Q_X = 1.5$, $Q_\alpha = 1$).

Thrust Level	D_{pt} [mm]	θ_{pt} [degrees]	δ_{ann} [mm]	Δp_{pt} [bar]	Δp_{ann} [bar]	L_{open} [mm]
1	19	0	0.70	1.77	1.0429	0.1020
2	-	-	-	2.82	1.6496	0.1283
3	-	-	-	3.90	2.2709	0.1505
4	-	-	-	4.92	2.8559	0.1688
5	-	-	-	6.00	3.2876	0.1880

Table 5. Theoretical performance of the optimized pintle injector.

Thrust Level	SMD [μm]	α [degrees]	X [mm]
1	9.4749	31.5106	4.6320
2	7.7679	34.8878	3.1984
3	6.6811	37.3687	2.4133
4	5.9621	39.2061	1.9503
5	5.6664	41.8715	1.6914

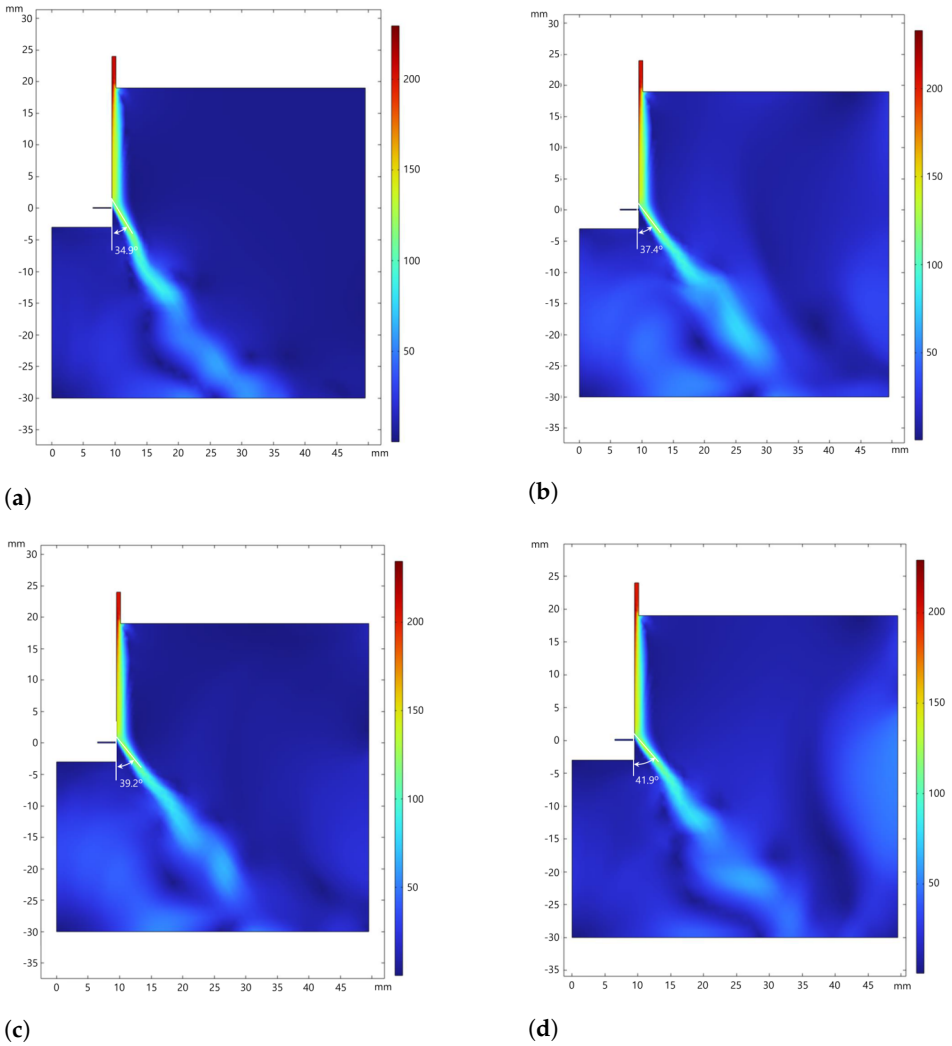

Figure 12. The spray angle simulation results by the thrust levels. (**a**) The spray angle result (34.9°) in thrust level 2; (**b**) the spray angle result (37.4°) in thrust level 3; (**c**) the spray angle result (39.2°) in thrust level 4; (**d**) the spray angle result (41.9°) in thrust level 5.

5. Conclusions

This study aimed to develop and demonstrate an optimization method for a pintle injector design. For this, we design a pintle injector for 1000 N thrust and 5 to 1 throttle ability liquid-propellant rocket engine (LPRE) with liquid oxygen and gaseous methane propellants. Then, we identify a set of design variables using an optimization method based on convex quadratic programming (CQP) to maximize performance with the relationships of the performance parameters. Through the optimization process, we can find the configuration of an optimal pintle injector for a specific project by applying the weight matrix (**Q**) in the cost function, and we check the impact of each of the weight factor (Q_i) values on the design variables. Then, we verify the performance of the optimization method with an example using a numerical simulation by COMSOL Multiphysics. Through this work, we can demonstrate the effectiveness of the optimization method for pintle injector design. The procedures can be found in more detail in Ref. [46].

Author Contributions: Conceptualization, J.C., E.A. and A.B.; methodology, J.C. and E.A.; software, J.C. and E.A.; validation, J.C. and E.A.; resources, J.C.; preparation of the initial draft, J.C., E.A. and A.B.; modifications and revisions, J.C. All authors have read and agreed to the published version of the manuscript.

Funding: This research received European Regional Development Fund in Kiruna, Sweden.

Institutional Review Board Statement: Not applicable.

Informed Consent Statement: Not applicable.

Data Availability Statement: Not applicable.

Acknowledgments: We are thankful for support through the RIT (Space for Innovation and Growth) project/European Regional Development Fund in Kiruna, Sweden.

Conflicts of Interest: The authors declare no conflict of interest.

References

1. Gilroy, R.; Sackheim, R. The Lunar module descent engine-a historical summary. In Proceedings of the 25th Joint Propulsion Conference, Monterey, CA, USA, 10–12 July 1989; p. 2385.
2. Betts, E.; Frederick, R. A historical systems study of liquid rocket engine throttling capabilities. In Proceedings of the 46th AIAA/ASME/SAE/ASEE Joint Propulsion Conference & Exhibit, Nashville, TN, USA, 25–28 July 2010; p. 6541.
3. Casiano, M.J.; Hulka, J.R.; Yang, V. Liquid-propellant rocket engine throttling: A comprehensive review. *J. Propuls. Power* **2010**, *26*, 897–923. [CrossRef]
4. Choo, K.; Mun, H.; Nam, S.; Cha, J.; Ko, S. A survey on recovery technology for reusable space launch vehicle. *J. Korean Soc. Propuls. Eng.* **2018**, *22*, 138–151. [CrossRef]
5. Muelhaupt, T.J.; Sorge, M.E.; Morin, J.; Wilson, R.S. Space traffic management in the new space era. *J. Space Saf. Eng.* **2019**, *6*, 80–87. [CrossRef]
6. Kuntanapreeda, S.; Hess, D. Opening access to space by maximizing utilization of 3D printing in launch vehicle design and production. *Appl. Sci. Eng. Prog.* **2021**, *14*, 143–145. [CrossRef]
7. Yao, Z.; Qi, Y.; Bao, W.; Zhang, T. Thrust Control Method and Technology of Variable-Thrust Liquid Engine for Reusable Launch Rocket. *Aerospace* **2022**, *10*, 32. [CrossRef]
8. Austin, B.L.; Heister, S.; Anderson, W. Characterization of pintle engine performance for nontoxic hypergolic bipropellants. *J. Propuls. Power* **2005**, *21*, 627–635. [CrossRef]
9. Bedard, M.; Feldman, T.; Rettenmaier, A.; Anderson, W. Student design/build/test of a throttleable LOX-LCH4 thrust chamber. In Proceedings of the 48th AIAA/ASME/SAE/ASEE Joint Propulsion Conference & Exhibit, Atlanta, GA, USA, 30 July 2012–1 August 2012; p. 3883.
10. Fang, X.-x.; Shen, C.-b. Study on atomization and combustion characteristics of LOX/methane pintle injectors. *Acta Astronaut.* **2017**, *136*, 369–379. [CrossRef]
11. Son, M.; Radhakrishnan, K.; Yoon, Y.; Koo, J. Numerical study on the combustion characteristics of a fuel-centered pintle injector for methane rocket engines. *Acta Astronaut.* **2017**, *135*, 139–149. [CrossRef]
12. Radhakrishnan, K.; Son, M.; Lee, K.; Koo, J. Effect of injection conditions on mixing performance of pintle injector for liquid rocket engines. *Acta Astronaut.* **2018**, *150*, 105–116. [CrossRef]
13. Dai, J.; Yu, H. Numerical and experimental investigations of geometrical parameters on GH2/GO2 injector. *Aerosp. Sci. Technol.* **2020**, *106*, 106187. [CrossRef]

14. Son, M.; Lee, K.; Koo, J. Characteristics of anchoring locations and angles for GOX/GCH4 flames of an annular pintle injector. *Acta Astronaut.* **2020**, *177*, 707–713. [CrossRef]
15. Zhang, Y.; Yu, N.; Tian, H.; Li, W.; Feng, H. Experimental and numerical investigations on flow field characteristics of pintle injector. *Aerosp. Sci. Technol.* **2020**, *103*, 105924. [CrossRef]
16. Zhao, F.; Zhang, H.; Zhang, H.; Bai, B.; Zhao, L. Review of atomization and mixing characteristics of pintle injectors. *Acta Astronaut.* **2022**, *200*, 400–419. [CrossRef]
17. Zhou, R.; Shen, C. Experimental study on the spray characteristics of a pintle injector element. *Acta Astronaut.* **2022**, *194*, 255–262. [CrossRef]
18. Jin, X.; Yang, Y.; Cao, X.; Wu, J. Effect of Local Momentum Ratio on Spray Windward Distribution of a Gas–Liquid Pintle Injector Element. *Aerospace* **2022**, *9*, 494. [CrossRef]
19. Son, M.; Radhakrishnan, K.; Koo, J.; Kwon, O.C.; Kim, H.D. Design Procedure of a movable pintle injector for liquid rocket engines. *J. Propuls. Power* **2017**, *33*, 858–869. [CrossRef]
20. Erkal, B.; Sumer, B.; Aksel, M.H. Design and Cold Flow Experiment Procedure of a Pintle Injector. In Proceedings of the AIAA Propulsion and Energy 2019 Forum, Indianapolis, IN, USA, 19–22 August 2019; p. 4117.
21. Rajendran, R.; Prasad, S.; Subhashree, S.; Phutane, T.S.; Saoor, V.S. Design and optimization of pintle injector for liquid rocket engine. *Int. J. Eng. Appl. Sci. Technol.* **2020**, *5*, 151–159. [CrossRef]
22. Sutton, G.P.; Biblarz, O. *Rocket Propulsion Elements*; John Wiley & Sons: Hoboken, NJ, USA, 2016.
23. Son, M. Correlations between Spray and Combustion Characteristics of a Movable Pintle Injector for Liquid Rocket Engines. Ph.D. Thesis, Department of Aerospace and Mechanical Engineering, Korea Aerospace University, Goyang, Republic of Korea, 2017.
24. Hill, P.G.; Peterson, C.R. *Mechanics and Thermodynamics of Propulsion*; Addison-Wesley: Boston, MA, USA, 1992.
25. Vasques, B.B.; Haidn, O.J. Effect of pintle injector element geometry on combustion in a liquid oxygen/liquid methane rocket engine. In Proceedings of the 7th European Conference for Aeronautics and Space Sciences (EUCASS), Milan, Italy, 3–6 July 2017; p. 88.
26. Kowalczuk, P.B.; Drzymala, J. Physical meaning of the Sauter mean diameter of spherical particulate matter. *Part. Sci. Technol.* **2016**, *34*, 645–647. [CrossRef]
27. Dressler, G.; Bauer, J. TRW pintle engine heritage and performance characteristics. In Proceedings of the 36th AiAA/ASME/SAE/ASEE Joint Propulsion Conference and Exhibit, Las Vegas, NV, USA, 24–28 July 2000; p. 3871.
28. Quan, S.; Schmidt, D.P. Direct numerical study of a liquid droplet impulsively accelerated by gaseous flow. *Phys. Fluids* **2006**, *18*, 102103. [CrossRef]
29. Gordon, S.; McBride, B.J. *Computer Program for Calculation of Complex Chemical Equilibrium Compositions and Applications. Part 1: Analysis*; Technical Report; NASA Lewis Research Center: Cleveland, OH, USA, 1994.
30. Martins, J.R.; Ning, A. *Engineering Design Optimization*; Cambridge University Press: Cambridge, UK, 2021.
31. Cai, G.; Fang, J.; Xu, X.; Liu, M. Performance prediction and optimization for liquid rocket engine nozzle. *Aerosp. Sci. Technol.* **2007**, *11*, 155–162. [CrossRef]
32. Yelchuru, R.; Skogestad, S. Convex formulations for optimal selection of controlled variables and measurements using mixed integer quadratic programming. *J. Process. Control* **2012**, *22*, 995–1007. [CrossRef]
33. Bartlett, R.A.; Biegler, L.T.; Backstrom, J.; Gopal, V. Quadratic programming algorithms for large-scale model predictive control. *J. Process. Control* **2002**, *12*, 775–795. [CrossRef]
34. Corke, P.I.; Khatib, O. *Robotics, Vision and Control: Fundamental Algorithms in MATLAB*; Springer: Berlin/Heidelberg, Germany, 2011; Volume 73.
35. Zhang, Z.; Li, J.; Wang, J. Sequential convex programming for nonlinear optimal control problems in UAV path planning. *Aerosp. Sci. Technol.* **2018**, *76*, 280–290. [CrossRef]
36. Jo, B.U.; Ahn, J. Near time-optimal feedback instantaneous impact point (IIP) guidance law for rocket. *Aerosp. Sci. Technol.* **2018**, *76*, 523–529. [CrossRef]
37. Jouini, T.; Rantzer, A. On cost design in applications of optimal control. *IEEE Control Syst. Lett.* **2021**, *6*, 452–457. [CrossRef]
38. Cha, J.; de Oliveira, É.J. Robust Guidance and Control of Liquid-Propellant Rocket Engines for Landing of Reusable Stages using Fuzzy PID Control. In Proceedings of the 72th International Astronautical Congress (IAC), Dubai, United Arab Emirates, 25–29 October 2021.
39. Mercieca, E. Spray Characteristics in Gas/Liquid Pintle Injection. Master's Thesis, Department of Aerospace Engineering, Delft University of Technology, Delft, The Netherlands, 2017.
40. Huzel, D.K.; Huang, D.H. *Modern Engineering for Design of Liquid-Propellant Rocket Engines*; AIAA: San Diego, CA, USA, 1992; Volume 147.
41. Nelson, K.; Hawk, C. *Experimental Investigation of an Integrated Strut-Rocket/Scramjet Operating at Mach 4.0 and 6.5 Conditions*; Jannaf Propulsion Meeting: Cleveland, OH, USA, 1998.
42. Pennington, D.; Man, T.; Persons, B. *Rocket Propulsion Hazard Summary: Safety Classification, Handling Experience and Application to Space Shuttle Payload*; Technical Report; NASA: Washington, DC, USA, 1977.
43. Osipov, V.; Muratov, C.; Hafiychuk, H.; Ponizovskaya-Devine, E.; Smelyanskiy, V.; Mathias, D.; Lawrence, S.; Werkheiser, M. Hazards Induced by Breach of Liquid Rocket Fuel Tanks: Conditions and Risks of Cryogenic Liquid Hydrogen-Oxygen Mixture Explosions. *arXiv* **2010**, arXiv:1012.5135.

44. Chen, Y.; Liu, X.; Wang, J. Effects of Reversed Shock Waves on Operation Mode in H_2/O_2 Rotating Detonation Chambers. *Energies* **2021**, *14*, 8296. [CrossRef]
45. Multiphysics, C. *Introduction to COMSOL Multiphysics*; COMSOL Multiphysics: Burlington, MA, USA, 2016.
46. Andersson, E. Numerical Approach to the Design and Optimisation of a Bi-Propellant Pintle Injector. Master's Thesis, Department of Computer Science, Electrical and Space Engineering, Space Technology, Luleå University of Technology, Kiruna, Sweden, 2022.